Project Report

ETS-4

L. G. Taff

Observing Artificial Satellites

8 October 1976

Prepared for the Department of the Air Force
under Electronic Systems Division Contract F19628-76-C-0002 by

Lincoln Laboratory

MASSACHUSETTS INSTITUTE OF TECHNOLOGY

LEXINGTON, MASSACHUSETTS

The work reported in this document was performed at Lincoln Laboratory, a center for research operated by Massachusetts Institute of Technology, with the support of the Department of the Air Force under Contract F19628-76-C-0002.

This technical report has been reviewed and is approved for publication.

FOR THE COMMANDER

Raymond L. Loiselle

Raymond L. Loiselle, Lt. Col., USAF
Chief, ESD Lincoln Laboratory Project Office

MASSACHUSETTS INSTITUTE OF TECHNOLOGY
LINCOLN LABORATORY

OBSERVING ARTIFICIAL SATELLITES

L. G. TAFF
Group 94

PROJECT REPORT ETS-4

8 OCTOBER 1976

LEXINGTON MASSACHUSETTS

ABSTRACT

This report describes a technique that can be used to derive the penalty paid, in terms of increased apparent magnitude, for not observing artificial satellites at their maximum diffuse brightness. The procedure is applied here to the simple case of geostationary right-circular cylinders. We find that if these satellites (at their brightest) are $0\overset{m}{.}5$ brighter than the system limit, then ≈ 63 percent of all such satellites within 60 degrees of the GEODSS ETS will <u>never</u> be visible.

I. Introduction

This report explores the visibility of a geostationary satellite with respect to the time of observation and the difference between the longitude of the sub-satellite point and the longitude of the observer's meridian ($\Delta\lambda$). The analysis illustrates a versatile technique applicable to any distribution of satellite orbits, shapes, sizes, reflectivities, orientations, and motions about the satellite center of mass. In particular, the penalty paid, in terms of the increased apparent magnitude (Δm), is revealed as a function of the time of observation and $\Delta\lambda$. The calculations are restricted to diffuse reflections.

The next section more fully specifies the problem and the third presents the findings of the computations in a series of graphs. Additional numerical details are in the Appendix.

II. Specifications

A. Orbits

All satellites are in a circular orbit with period $P = 1$ mean sidereal day, geocentric declination = 0, and geocentric distance $r = 42164.3$ km $= (GM_{\oplus}P^2/4\pi^2)^{1/3}$.

B. Size, Shape, and Reflectivity

All satellites are right circular cylinders with uniform reflectivity. They all have the same dimensions and reflect diffusely. Hence, their phase function is (Giese 1963, McCue et al. 1971)

$$F = \cos\delta'\cos\delta'_{\odot}[(\pi - \theta)\cos\theta + \sin\theta]/\pi, \quad (1a)$$

$$\theta = (|\alpha' - \alpha'_{\odot}| - 12^h), \quad (1b)$$

where primed quantities denote topocentric coordinates. See Figure 1.

C. Orientation and Motion About the Center of Mass

The angular momentum vector is parallel to the angular velocity vector and both point towards the North Celestial Pole. The motion is stable and the angular speed in constant.

D. Satellite Population

It is assumed that an ensemble of identical satellites are uniformly distributed in $\Delta\lambda$ (measured positive to the east). The extreme values for $\Delta\lambda$ used here correspond to topocentric zenith distances of 60° and 70°. When apparent magnitudes are indicated instead of Δm, it is assumed that a satellite due south

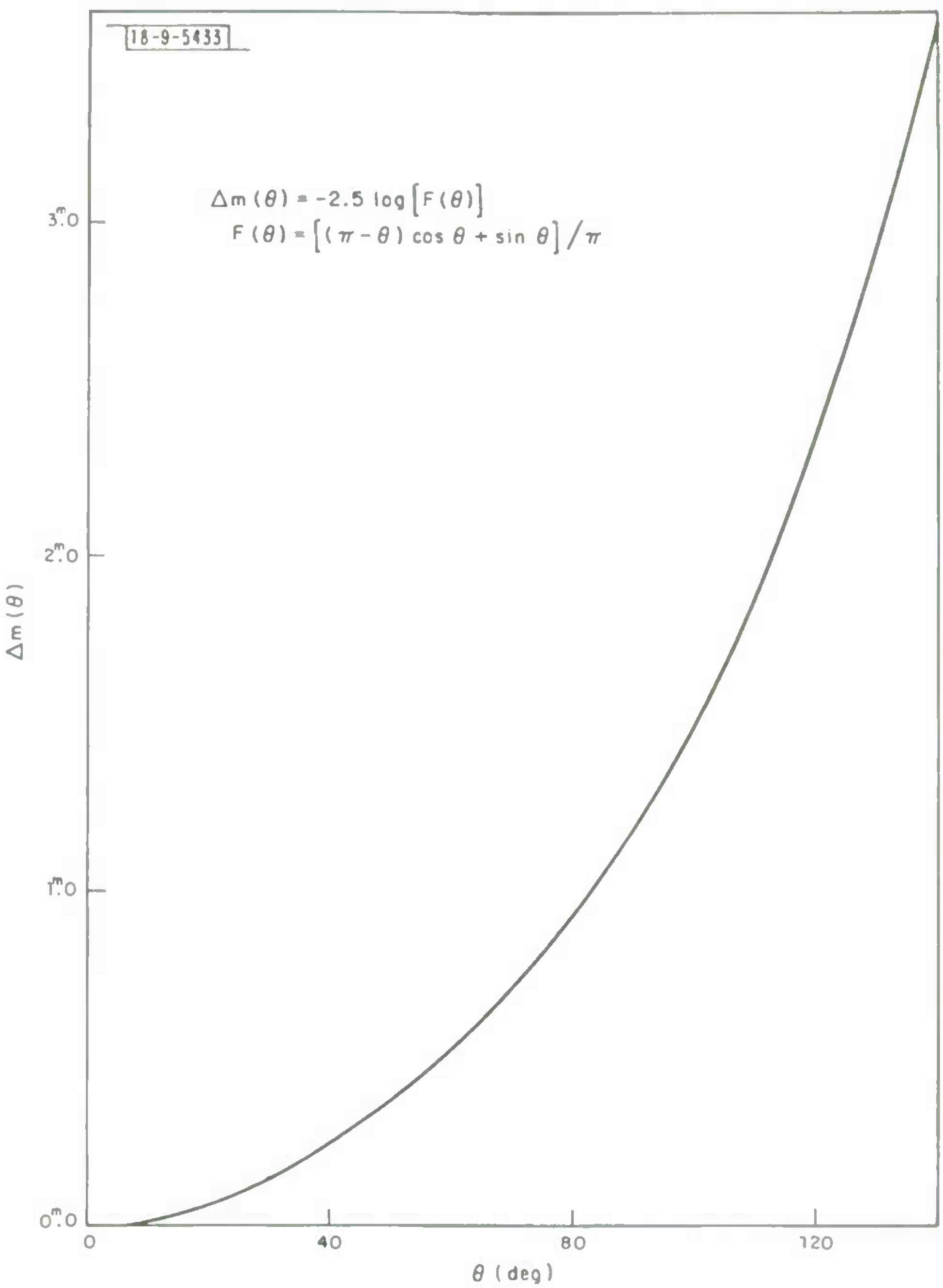

Fig. 1. Phase function for a diffusely reflecting cylinder.

of the observer (i. e., the GEODSS ETS) when viewed at full phase through an atmosphere with $\varepsilon = 0\overset{m}{.}25$/air mass extinction has an apparent magnitude of exactly 16^{m}.

E. Times of the Year and of the Night

For this satellite population there are four interesting times of the year. They are (i) at an equinox when eclipses occur, (ii) near the eclipse season when they are the brightest, (iii) at a solstice when they are faintest, and (iv) in between the solstice and the near equinox times. All calculations presented here for these four periods represent three week averages of the days numbered 59-79, 80-100, 161-181, and 120-140 inclusive. Since a satellite's brightness is not symmetrical about local apparent (or mean) solar midnight, when hours from midnight is used the results represent an average of the pre-and post-midnight hours.

F. Procedure

The apparent magnitude of each satellite in the ensemble was computed on the hour between sunset (6 PM local mean solar time = T) and sunrise (6 AM) inclusive for every day of the four three week periods. These results when then combined to yield Figures 2-8.

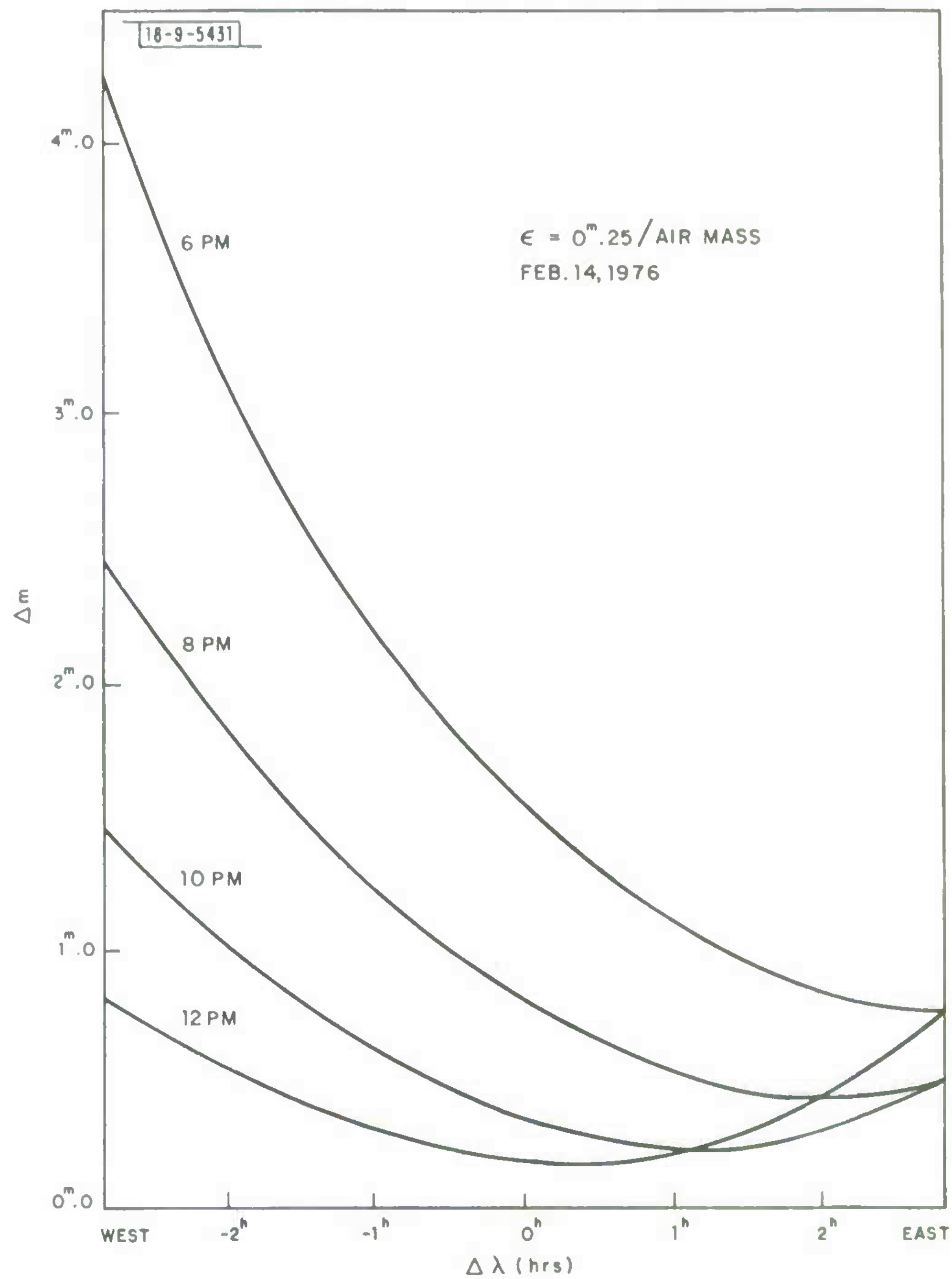

Fig. 2. Magnitude loss at 6PM(2)12PM as a function of sub-satellite-meridian longitude for geostationary cylinders.

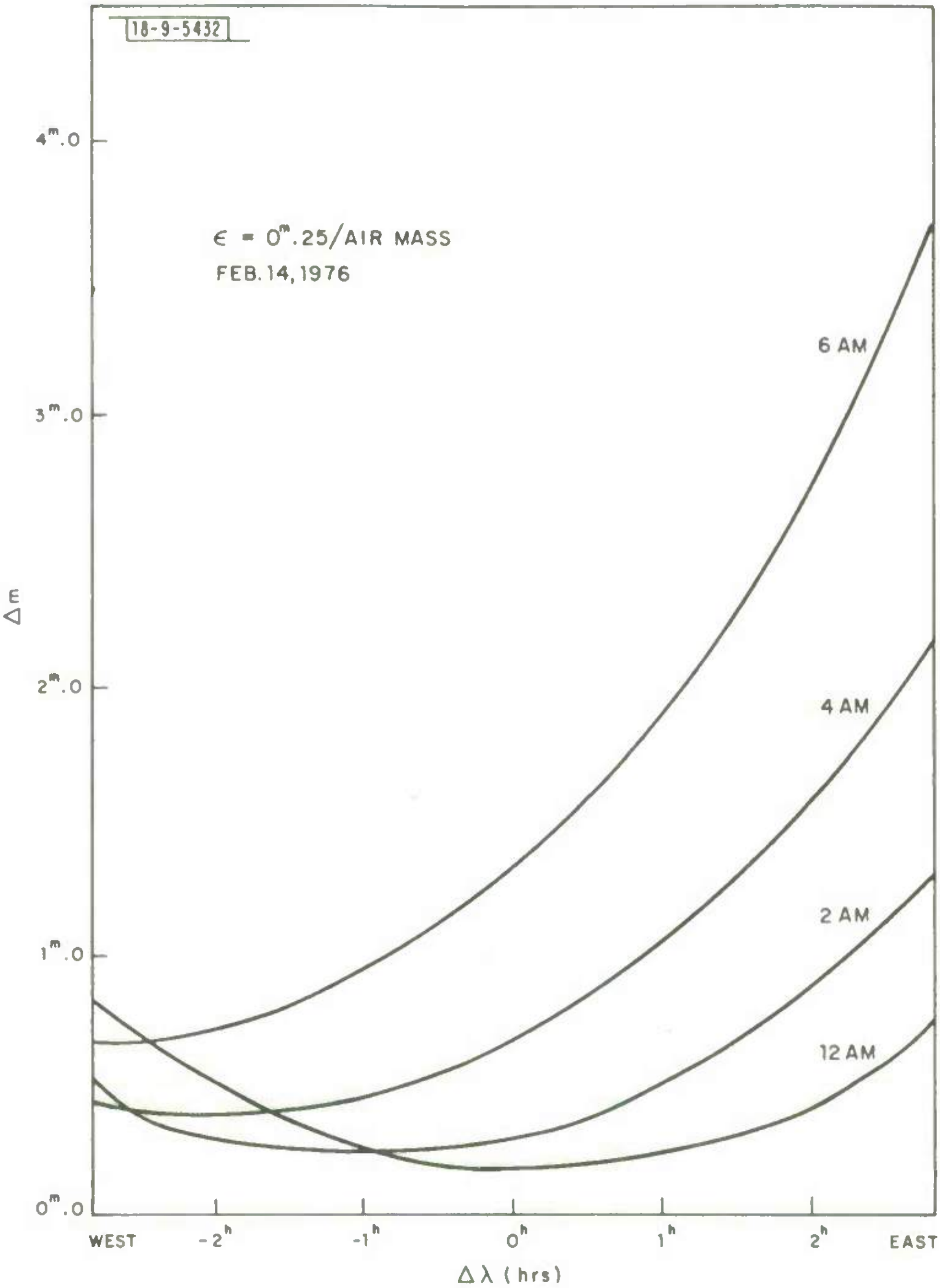

Fig. 3. Magnitude loss at 0(2)6AM as a function of sub-satellite-meridian longitude for geostationary cylinders.

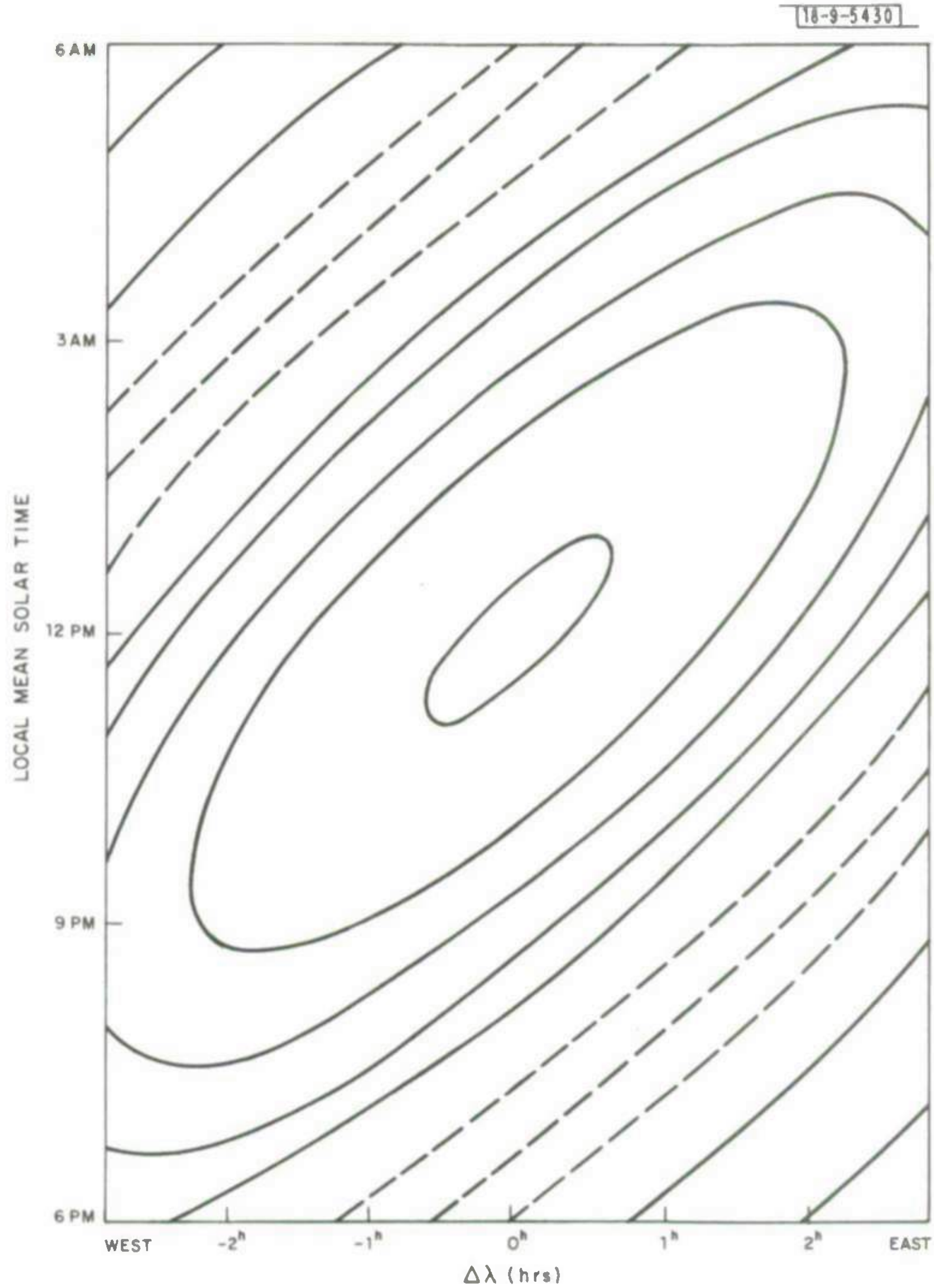

Fig. 4. Contours of constant Δm for the winter solstice. Curves show successive magnitude loss of 0.250(0.125)0.750(0.25)1.50(0.5)2.5.

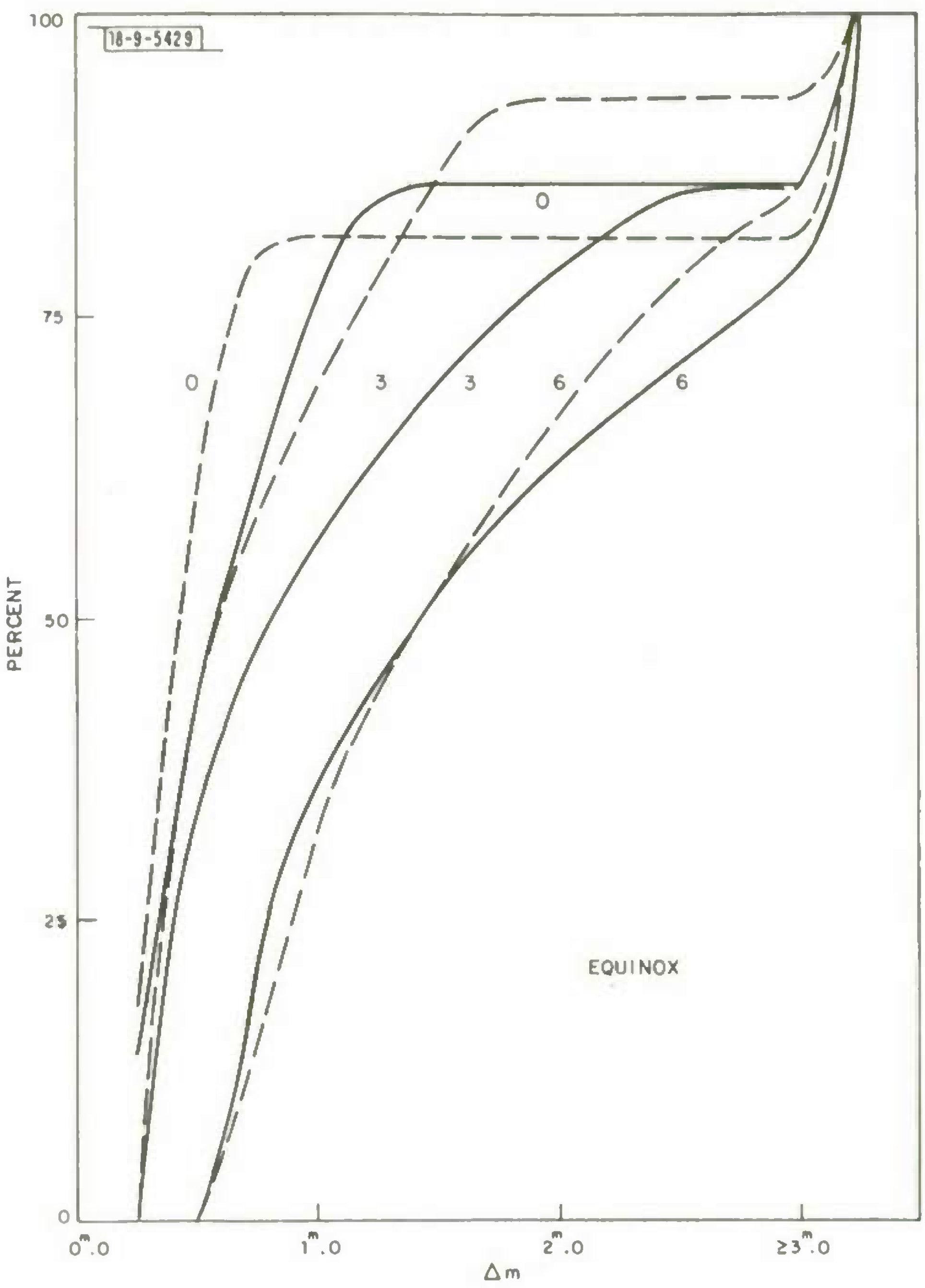

Fig. 5. Three week average of magnitude loss for a uniform distribution of geostationary satellites at an equinox.

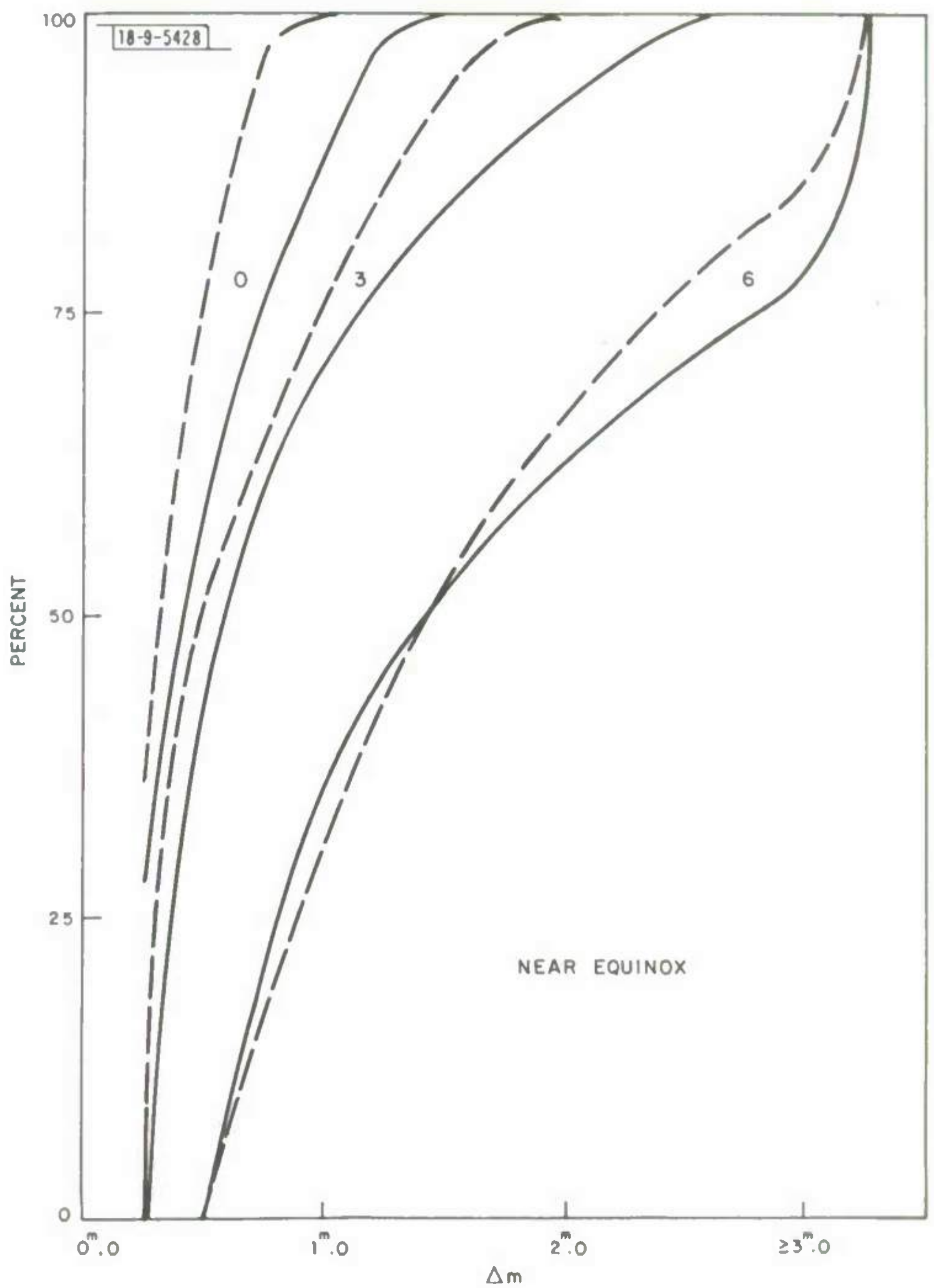

Fig. 6. Three week average of magnitude loss for a uniform distribution of geostationary satellites near the equinox.

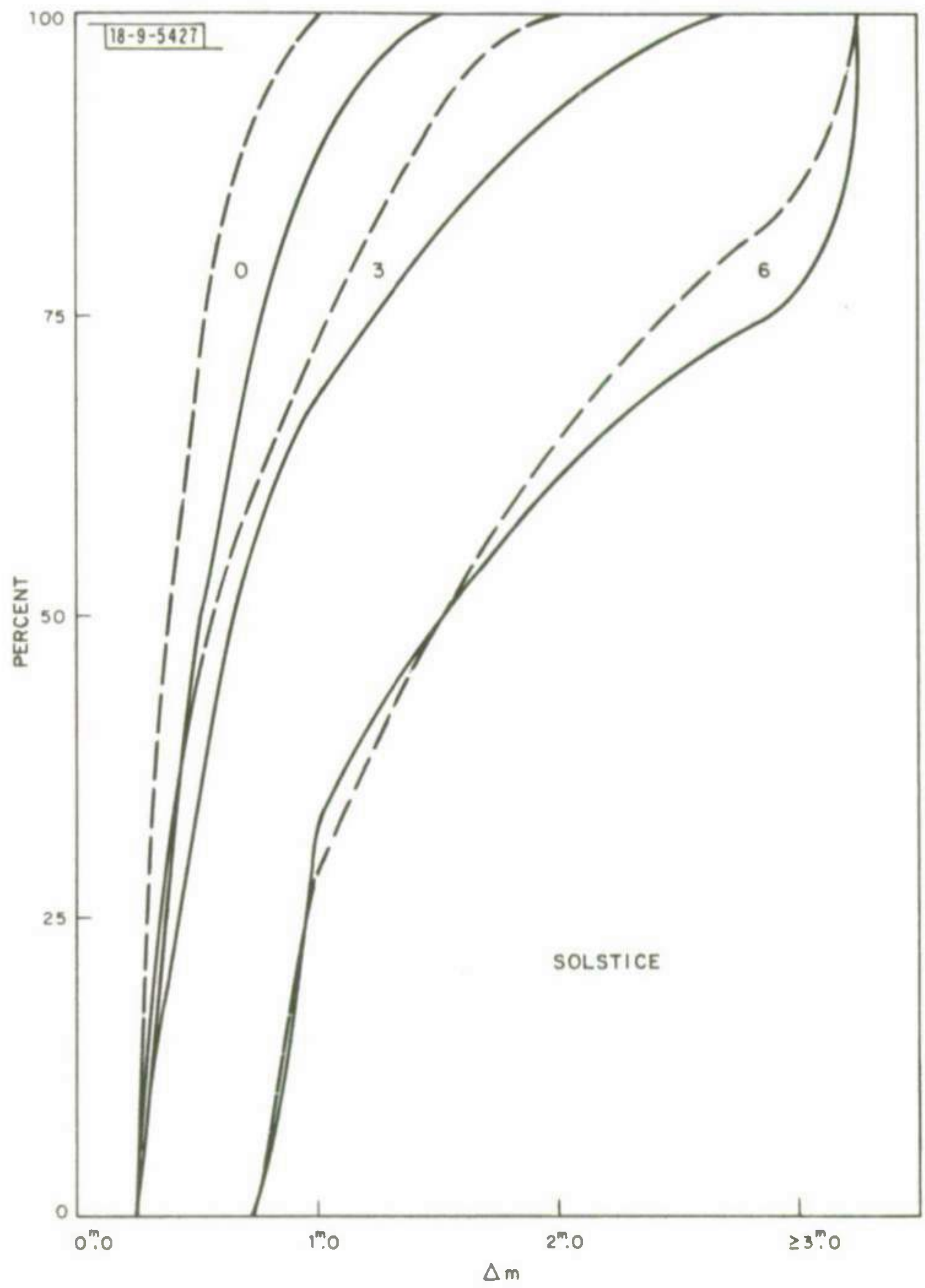

Fig. 7. Three week average of magnitude loss for a uniform distribution of geostationary satellites at a solstice.

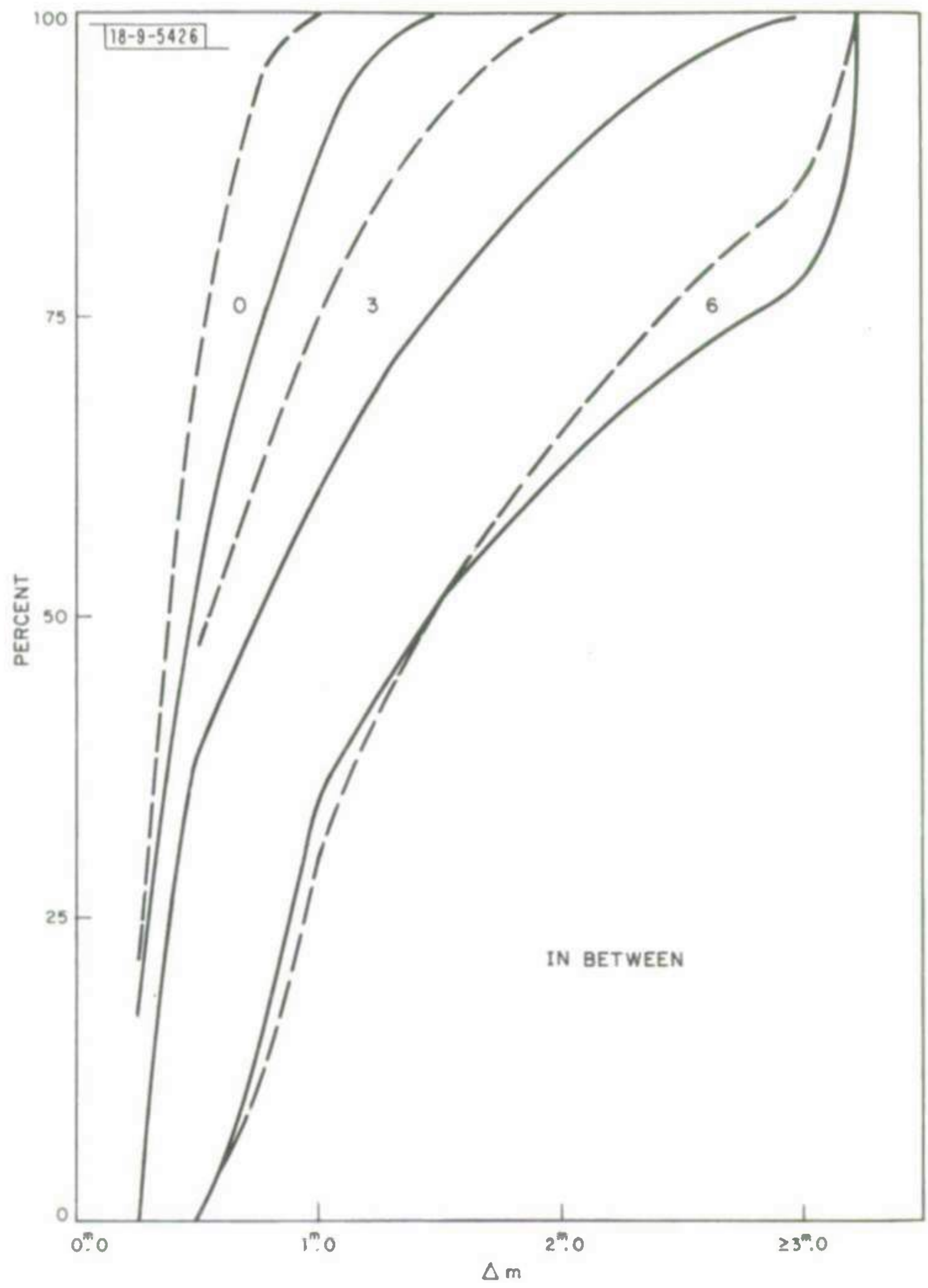

Fig. 8. Three week average of magnitude loss for a uniform distribution of geostationary satellites in between equinox and solstice.

III. Results

Figures 2 and 3 show the loss of brightness, in magnitudes, from maximum brightness as a function of $\Delta\lambda$ at T = 18(2)30. As one would expect satellites in the west at sunset are very faint etc., and the curves are almost symmetrical about T = 24. Note, however, that even at 8 PM the loss at the 60° zenith distance limit is $\Delta m = 2\overset{m}{.}5$.

Figure 4 is a plot of constant Δm contours in a T - $\Delta\lambda$ plane. The solid (innermost) curves represent losses in steps of $0\overset{m}{.}125$ starting from $\Delta m = 0\overset{m}{.}250$. The dotted curves represent successive losses in steps of $0\overset{m}{.}25$ starting at $\Delta m = 1\overset{m}{.}00$ and the solid (outermost) curves represent losses in steps of $0\overset{m}{.}5$ starting at $\Delta m = 2\overset{m}{.}0$. An example of the use of such a graph is to calculate the fraction of the area displayed within a given Δm value. Thus, the area enclosed by $\Delta m = 0\overset{m}{.}50$ is approximately 37 percent of the total. Hence, an automatic detection system whose limit is $m = 16\overset{m}{.}5$ (<u>independent</u> of the signal-to-noise ratio) would lose, <u>a priori</u>, 2/3 of this population.

Figures 5-8 show the cumulative number of satellites (in percent units) with magnitude loss $\leq \Delta m$ for Δm = 0(0.25)2.75, $\geq$ 3 at the four different times of the year. Each figure contains curves for 0(3)6 hours from midnight for both the 60° (solid) and 70° (dotted) zenith distance limits. The effects of eclipses at the equinoxes and losses due to larger air mass are clearly visible.

A simple extrapolation of these results can be made for any phase function that decreases more rapidly with θ [cf. Eqs. (1)], namely that the restrictions on observing become more stringent and the penalty paid becomes larger.

Appendix

In this appendix we discuss the calculation of the satellite brightnesses used in the preceding analysis. All of the calculations refer to the GEODSS ETS whose geodetic coordinates are

$$\text{height above geoid} = 1.529382768 \text{ km},$$

$$\text{geodetic latitude} = +33\overset{\circ}{.}81805667 = \phi$$

$$\text{geodetic longitude} = 253\overset{\circ}{.}341415028\text{E} = \lambda.$$

The corresponding geocentric values are

$$\text{geocentric distance} = 6373.103 \text{ km} = \rho,$$

$$\text{geocentric latitude} = +33\overset{\circ}{.}64037171 = \phi'.$$

If T is the local mean solar time and t is the local mean universal time then

$$T = t + \lambda - 24 = t - 7\overset{h}{.}1105723.$$

Although local apparent solar time would be more appropriate than local mean solar time, as the equation of time is $\leq 16^m$, it's not an important effect. The local mean sidereal time, τ, is related to t by (for 1976)

$$\tau = 1\overset{h}{.}0027379t + 6\overset{h}{.}5709822 \times 10^{-2}D - 0\overset{h}{.}52409761,$$

where $t \in [0, 24)$ and D is the integral number of days elapsed since 0^h UT on 0 January 1976.

The position of the sun is calculated based on the two assumptions (i) that the ecliptic latitude of the sun is zero and (ii) that its motion is strictly Keplerian. Therefore, if e is the eccentricity of the orbit, T_p is the time of perigee passage, and ω is the argument of perigee then

$$\lambda_\Theta = v + \omega,$$

$$v \simeq M + (2e - e^3/4)\sin M + (5e^2/4 - 11e^4/24)\sin 2M$$

$$+ (13e^3/12)\sin 3M + (103e^4/96)\sin 4M,$$

$$M = n(t - T_p),\ n = 360^\circ/365\overset{d}{.}24219,$$

where λ_Θ is the ecliptic longitude of the sun. For 1976 $T_p \simeq 4^d 11^h 29^m$ ET, $\omega = 283\overset{\circ}{.}23931$, $e = 1.6719199 \times 10^{-2}$. The transformation to equatorial coordinates uses a value of the obliquity of the ecliptic $\varepsilon = 23\overset{\circ}{.}442404$.

The position of the satellite is specified by

$$\text{geocentric distance} = 42164.3 \text{ km} = r,$$

$$\text{geocentric right ascension} = \tau + \Delta\lambda = \alpha,$$

$$\text{geocentric declination} = 0 = \delta,$$

where $\Delta\lambda$ is the difference (measured positive to the east) between the longitude of the sub-satellite point and the observer's meridian.

Since the equation of the equinoxes is $\leq 1^s$, we commit no substantial error in using τ instead of local apparent sidereal time. The topocentric equatorial coordinates (corrected only for geocentric parallax) are given by

$$\alpha' = \alpha + \tan^{-1}[a\sin\Delta\lambda/(1 - a\cos\Delta\lambda)],$$

$$\delta' = \delta - \tan^{-1}[b/(1 - b\cot\gamma)],$$

$$\cot\gamma = \cot\phi'\sec[(\alpha - \alpha')/2]\cos[(\alpha - \alpha')/2 - \Delta\lambda],$$

$$r' = r\sin\gamma\csc(\gamma - \delta'),$$

where

$$a = (\rho/r)\cos\phi' = 1.2583659 \times 10^{-1},$$

$$b = (\rho/r)\sin\phi' = 8.3733500 \times 10^{-2}.$$

The geocentric zenith distance, z, is given by (since $\delta = 0$)

$$\cos z = \cos\phi\cos\Delta\lambda.$$

The topocentric zenith distance (corrected only for geocentric parallax) is given by

$$z' = z + \tan^{-1}\{n\sin(z - \gamma')/[1 - n\cos(z - \gamma')]\},$$

where

$$n = (\rho/r)\cos(\phi - \phi')\sec\gamma' = 1.5114869 \times 10^{-1}\sec\gamma',$$

and γ' is determined from the geocentric and topocentric azimuths (measured from south to west) via

$$A = -\sin^{-1}[\sin\Delta\lambda\csc z],$$

$$A' = A + \tan^{-1}[m\sin A/(1 - m\cos A)],$$

$$m = (\rho/r)\sin(\phi - \phi')\csc z = 4.6874195 \times 10^{-4}\csc z,$$

$$\tan\gamma' = \tan(\phi - \phi')\cos[(A' + A/2]\sec[(A' - A)/2].$$

Finally, topocentric zenith distance corrected for geocentric parallax and refraction is calculated via

$$z'' = z' - 58''.2\ \tan z'.$$

Table AI contains $\Delta\lambda$, z, z' as a function z'' for $z'' = 40(5)75^{\circ}$.

The apparent magnitude, m, of the satellite is determined from

$$m = m_{\Theta} + \varepsilon X - 2.5\log[pR^2F(\Phi)/\Delta^2(r')^2]$$

where m_{Θ} is the apparent magnitude of the sun, ε is the extinction per unit air mass, X is taken to be $\sec z''$, p is the albedo, R is the radius of the equivalent area sphere, F is the phase function of the phase angle $\Phi[F(0) = 1]$, and Δ is the sun-satellite distance

TABLE AI

TOPO AND GEOCENTRIC ZENITH DISTANCE

z''	z'	z	$\Delta\lambda$
40°	$40^{\circ}0'48''.9$	$34^{\circ}24'59''$	$0^{h}27^{m}13^{s}.7$
45°	$45^{\circ}0'58''.2$	$38^{\circ}51'47''$	$1^{h}21^{m}38^{s}.6$
50°	$50^{\circ}1'\ 9''.4$	$43^{\circ}21'22''$	$1^{h}55^{m}44^{s}.3$
55°	$55^{\circ}1'23''.2$	$47^{\circ}53'58''$	$2^{h}24^{m}47^{s}.9$
60°	$60^{\circ}1'40''.9$	$52^{\circ}29'51''$	$2^{h}51^{m}31^{s}.3$
65°	$65^{\circ}2'\ 5''.0$	$57^{\circ}\ 9'14''$	$3^{h}16^{m}58^{s}.6$
70°	$70^{\circ}2'40''.3$	$61^{\circ}52'24''$	$3^{h}41^{m}43^{s}.0$
75°	$75^{\circ}3'38''.1$	$66^{\circ}39'40''$	$4^{h}\ 6^{m}\ 4^{s}.9$

in A. U. Variations in Δ can cause at most a $\pm\ 0^{m}.0006$ change in m for geostationary satellites and its variation has been ignored. Since the satellites are all identical cylinders, p and R are superfluous variables. If α', δ' are the topocentric coordinates of the artificial satellite and α'_{Θ} and δ'_{Θ} are the similar coordinates for the sun then, including the effects of parallax but not the solar semi-diameter,

$$\cos\Phi \simeq -\cos\Phi' + \mu\sin^2\Phi',$$

where

$$\cos\Phi' = \sin\delta'\sin\delta'_{\Theta} + \cos\delta'\cos\delta'_{\Theta}\cos(\alpha' - \alpha'_{\Theta})$$

$\mu \simeq$ (mean equatorial horizontal solar parallax)/(mean equatorial horizontal satellite parallax) $= 2.8076 \times 10^{-4}$.

The phase function for a cylinder is [Eqs. (1)]

$$F = \cos\delta'\cos\delta'_{\Theta}[(\pi - \theta)\cos\theta + \sin\theta]/\pi,$$

$$\theta = \left|\,|\alpha' - \alpha'_{\Theta}| - 12^{h}\right|.$$

In all cases geocentric rather than topocentric solar coordinates have been used because the solar semi-diameter is much larger than the solar parallax. Wherever magnitudes are used instead of magnitude differences the normalization has been such that a satellite

seen at full phase would have apparent magnitude of $16\overset{m}{.}00$ at the telescope, when $\varepsilon = 0\overset{m}{.}25$. Thus,

$$m = 15\overset{m}{.}959 + \varepsilon X + 2.5\log\{[\sin\gamma\csc(\gamma - \delta')]^2/F\}.$$

Satellites are assumed to be eclipsed whenever they have entered the earth's penumbral shadow. This has a radius at r of $D = 9^\circ 8' 56\overset{''}{.}0$. Since the transit time from (entrance into penumbral shadow) to (entrance into umbral shadow) is $\simeq 2^m 10^s$ this is conservative. Clearly the coordinates of the eclipse center are $(\alpha_\odot + 12, - \delta_\odot)$. Hence the angular distance between the satellite and the eclipse center is given by

$$d = \sin^{-1}\{[\cos\delta\sin(\alpha - \alpha_\odot - 12)]^2 + [\cos\delta_\odot\sin\delta + \sin\delta_\odot\cos\delta\cos(\alpha - \alpha_\odot - 12)]^2\}^{1/2} \simeq [(\alpha - \alpha_\odot - 12)^2 + \delta_\odot^2]^{1/2}.$$

Eclipse occurs whenever $d \leq D$.

REFERENCES

1. R. N. Giese, S. A. O. Spec. Rep. No. 127 (1963).

2. G. A. McCue, J. G. Williams, and J. N. Morford, Planet. Space Sci. 19, 851 (1971).

REPORT DOCUMENTATION PAGE		READ INSTRUCTIONS BEFORE COMPLETING FORM
1. REPORT NUMBER ESD-TR-76-309	2. GOVT ACCESSION NO.	3. RECIPIENT'S CATALOG NUMBER
4. TITLE (and Subtitle) Observing Artificial Satellites		5. TYPE OF REPORT & PERIOD COVERED Project Report 6. PERFORMING ORG. REPORT NUMBER Project Report ETS-4
7. AUTHOR(s) Laurence G. Taff		8. CONTRACT OR GRANT NUMBER(s) F19628-76-C-0002
9. PERFORMING ORGANIZATION NAME AND ADDRESS Lincoln Laboratory, M. I. T. P.O. Box 73 Lexington, MA 02173		10. PROGRAM ELEMENT, PROJECT, TASK AREA & WORK UNIT NUMBERS Program Element No. 63428F Project No. 2128
11. CONTROLLING OFFICE NAME AND ADDRESS Air Force Systems Command, USAF Andrews AFB Washington, DC 20331		12. REPORT DATE 8 October 1976 13. NUMBER OF PAGES 26
14. MONITORING AGENCY NAME & ADDRESS (if different from Controlling Office) Electronic Systems Division Hanscom AFB Bedford, MA 01731		15. SECURITY CLASS. (of this report) Unclassified 15a. DECLASSIFICATION DOWNGRADING SCHEDULE

16. DISTRIBUTION STATEMENT (of this Report)

Approved for public release; distribution unlimited.

17. DISTRIBUTION STATEMENT (of the abstract entered in Block 20, if different from Report)

18. SUPPLEMENTARY NOTES

None

19. KEY WORDS (Continue on reverse side if necessary and identify by block number)

artificial satellites
satellite observation
space object identification

20. ABSTRACT (Continue on reverse side if necessary and identify by block number)

This report describes a technique that can be used to derive the penalty paid, in terms of increased apparent magnitude, for not observing artificial satellites at their maximum diffuse brightness. The procedure is applied here to the simple case of geostationary right-circular cylinders. We find that if these satellites (at their brightest) are $0^{\mathrm{m}}\!.5$ brighter than the system limit, then ≈63 percent of all such satellites within 60 degrees of the GEODSS ETS will never be visible.